# Characterization of Superfine Down Powder

**Weilin Xu, Xin Wang, Weigang Cui, Xuqiang Peng, Wenbin Li, Xin Liu**

*Wuhan University of Science and Engineering, Wuhan 430073, People's Republic of China*

Received 6 August 2007; accepted 21 August 2008
DOI 10.1002/app.29205
Published online 11 November 2008 in Wiley InterScience (www.interscience.wiley.com).

**ABSTRACT:** Superfine down powder was produced from down fiber after it was cut into short pieces and ground on a purpose-built machine. Scanning electron microscopy photographs showed that the down fiber was ground into particles with some fiber fragments and a large amount of rod-shaped ultrafine powder. Particle size distribution analysis indicated that the average size of the down powder was 1.546 μm. Fourier transform infrared analysis showed that the absorbing peaks around 1640, 1520, and 1230 $cm^{-1}$ were sharper than those of the down fiber. X-ray diffraction analysis revealed that the crystallinity of the superfine down powder was a little lower than that of the down fiber. Thermogravimetric analysis showed that the thermal stability decreased when the down fiber was ground into powder. Differential scanning calorimetry analysis showed that the intensity of the heat-absorbing peaks of the down powder was lower than that of the down fiber, so the down powder decomposed more readily than the down fiber. © 2008 Wiley Periodicals, Inc. J Appl Polym Sci 111: 2204–2209, 2009

**Key words:** down powder; SEM; particle size distribution; FTIR; TGA; DSC

## INTRODUCTION

Silk, wool, and down fiber are high-quality natural protein fibers that have been widely used as high-quality textile materials. Those fibers that cannot be spun have been widely developed into new products, such as biotechnological and biomedical products. However, 100% regenerated silk fiber has not been industrially produced because no proper spinning technology has been developed.[1,2] So that its properties are retained, silk is widely produced in a powder form by different methods.[2–6] Silk fibroin powder has already found utility in cosmetic materials and functional foods. Powdered silk fibroin is considered effective as an additive for cosmetic and pharmaceutical preparations because of its moderate moisture absorption and retention properties and its high affinity for human skin; actually, down powder also preserves these virtues. Silk powder is one of the useful physical forms of silk fibroin protein, which has some special properties in comparison with the fiber and silk film for biomaterial applications.[7,8] Silk powder is also applied in textile finishes and used to finish yarn-dyed cotton fabrics.[9] The fine silk powder is absorbed into the cotton fibers to create a soft hand. The fabric made from this offers good drape characteristics and moisture-absorbing properties.

*Correspondence to:* W. Xu (weilin-xu@hotmail.com).
Contract grant sponsor: National Natural Science Foundation of China; contract grant number: 50203009.




Usually, compared with inorganic fibers, polymer fibers have high strength, high break intensity, and high elongation, which make them very difficult to crush into fine powders. To get a fine silk powder, usually silk fibroin powders are produced by a special chemical pretreatment to destroy the chemical bonds and reduce the crystallinity.[5] High-energy irradiation has also been used to destroy the crystals.[4] After the pretreatment, silk fibroin fibers are dissolved in an aqueous calcium chloride solution at a high temperature, and this is followed by a dialysis treatment to remove the salt; they are then dehydrated, dried, and pulverized to yield a fine fibroin powder.[6–8] Recently, simpler methods, which do not include dissolution and dialysis processes for silk fibroin, have been proposed.[9,10] For example, a rotary blade mill was used to cut fibers with an average size of about 100 μm. Then, the roughly cut silk fibroin fibers were pulverized with a conventional ball mill. However, it took 12 h to produce the powder. Some researchers are also trying to develop wool films to wrap products.[10]

Down fiber is a very special material applied in different products. Very fine and high-quality down fiber is very valuable and expensive and is widely used in the padding of warmth-maintaining textiles. However, some low-quality down fiber is very cheap and currently is wasted. To develop new products from abundant wasted down fiber, it is necessary to develop a superfine powder. This powder can be used for some polymer modification to improve properties such as the dyeing properties, moisture-absorbing properties, and degradation properties.

As stated previously, there are many common virtues of silk fiber and down fiber; it is believed that down powder can replace silk powder in some areas. So far, there is very little literature reporting the production of down powder and its properties when it is developed into a superfine powder. Previously, we developed an instrument and a special method to produce superfine wool powder.[11,12] In this study, a superfine down powder was produced with the developed method. It was much finer than some other organic powders, such as silk powder and ramie powder, which has been developed by some other researchers and mostly has an average size around 5–10 μm.[3–6] The color of the down fiber powder is white because the powder is produced at room temperature. In this article, some results from the characterization of the down powder are reported.

## EXPERIMENTAL

### Powder preparation

Down fibers peeled from ducks were supplied by Maolongwuzhong Down Co., Ltd. (Shaoxing, China). The diameter of the down fibers was around 25 μm. The down fibers were cut into short pieces (ca. 3 mm) with a rotary blade. They were then pretreated with a 0.5% NaClO (analytical-grade; Bodi Chemical Co., Ltd., Tianjin, China) solution at room temperature. After excessive water was removed, the down powder was ground between two milling pans. Details of the instruments and the methodology are available in refs. 11 and 12. The mills had special properties such as very low heat generation and high antiabrasion properties. The fiber pieces could be easily crushed into a fine powder under the mechanical action, which included pressure, drawing, torsion, and sheer action. After the powder was crushed for about 20 h, it was available for other applications.

### Scanning electron microscopy (SEM) analysis

SEM analysis was carried out with a scanning electron microscope (X-650, Hitachi, Tokyo, Japan) at a 10-kV acceleration voltage after the samples were sputter-coated with a 10–15-nm layer of gold.

### Powder size distribution testing

A laser particle analyzer (JL-1166, Chengdu Jingxin Powder Analyzer Instrument Co., Ltd., Chengdu, China) was used to measure the average particle size and distribution of the superfine down powder. The powder was ultrasonically dispersed in distilled water. The powder solution was circled through the laser testing zone, and diameter data were collected and analyzed with computer software.

### Fourier transform infrared (FTIR) analysis

FTIR spectra of the down fiber and down powder were obtained on a Tensor 27 spectrometer (Bruker Optics, Inc., Billerica, MA). The absorbance of ATR spectra of the samples between 600 and 4000 $cm^{-1}$ was collected by 32 scans for each spectrum, and the resolution of the ATR spectra was 4 $cm^{-1}$.

### X-ray diffraction analysis

In the X-ray diffraction analysis, the samples were dispersed onto a stub and placed within the chamber of an analytical X-ray powder diffractometer (Damax-rA, Rigaku Corp., Tokyo, Japan, wavelength = 1.54 Å, CuKa radiation) with a generator intensity of 40 kV and a generator current of 50 mA. The samples were then scanned from $2\theta = 3°–60°$ in steps of 0.02°.

### Thermal analysis

Thermogravimetry (TG) was performed on a TG 209 F1 tester (Netzsch, Bavaria, Germany), which was nitrogen-protected, at a heating rate of 20°C/min. Differential scanning calorimetry (DSC) was performed on a model DSC 204F1 system (Netzsch) at a heating rate of 20°C/min. The open aluminum cell was swept with nitrogen gas during the analysis.

## RESULTS AND DISCUSSION

### SEM photographs

SEM photographs of the down fiber and powder are shown in Figure 1. Figure 1(a) shows a typical down fiber at the untreated stage; unlike the other protein fiber, there is a main trunk, with the most fine fiber [with a diameter of ca. 10 μm, as Fig. 1(b) shows] embedded around the fiber. Figure 1(c,d) shows the morphology of the superfine down powder; although some short fiber residues can be seen in the micrographs, most of the powder particles are round rather than fibrous.

From Figure 1, it is apparent that the down fibers were cut and split into small pieces, with some fiber fragments and a large number of ultrafine particles. Most particles showed a rod shape rather than a globular shape. This rod shape indicates the different application fields of the superfine powder, such as composite fillers and water-absorbent paths in membranes. In the process of grinding, fibers were first destroyed in the amorphous region, and some crystals were also broken.[13] The diameters of most of the powder were less than 10 μm; at this stage,

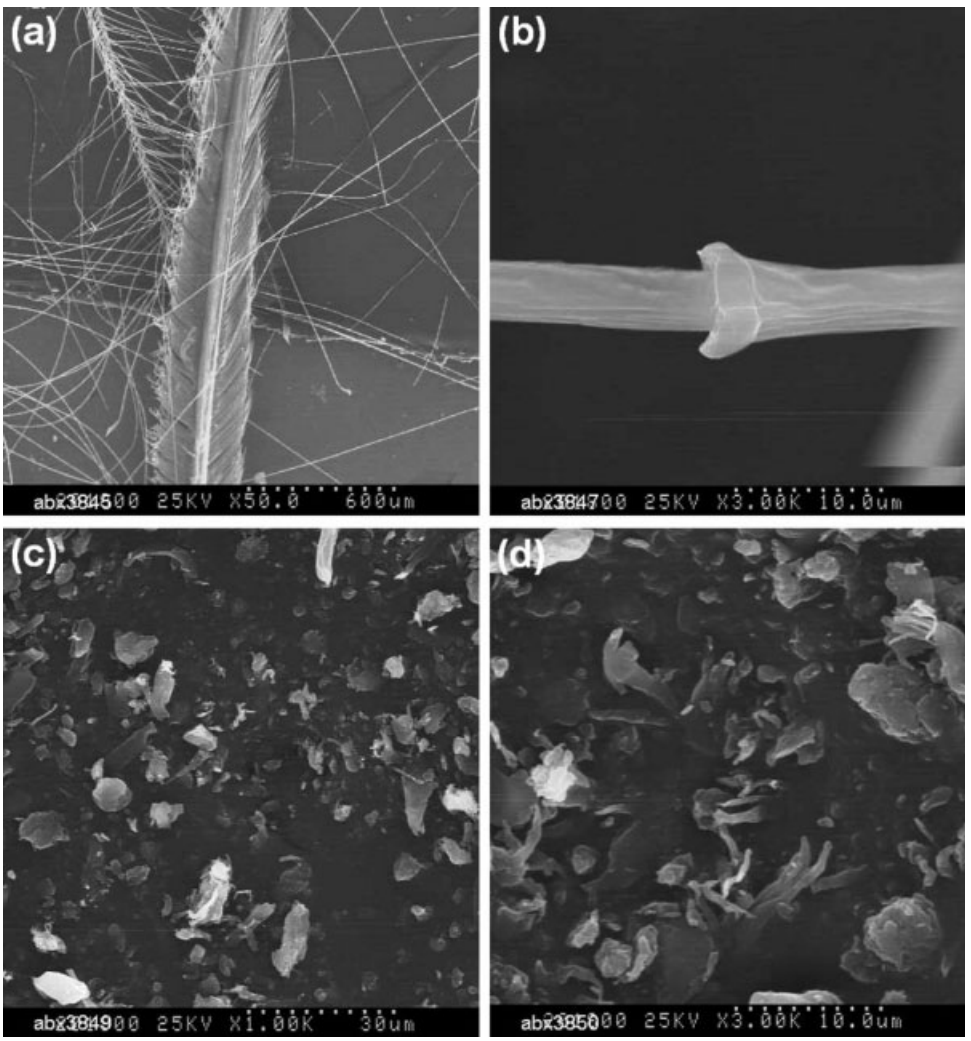


**Figure 1** SEM photographs of down fiber and down powder: (a) down fiber; (b) a typical fine fiber, and (c,d) down powder at different magnifications.

there were some small crystals in the powder, which may have preserved some of the original properties of the down fiber.

### Down powder size distribution

Because SEM photographs just showed images of the down powder in a specific area, a laser particle analyzer was used to perform a quantitative analysis of the actual particle size distribution of the powder. Figure 2 shows the powder size distribution of the down powder from 0 to 13 μm; the majority of the powder was distributed around 0–3 μm, some was distributed from 3 to 10 μm, and a little of the powder was distributed over 10 μm. After calculations with the data from Figure 2, we found that 24.7% and 41.3% of the powder were distributed under 1 μm and 2 μm, respectively. Thus, the powder was largely on a microscale.

Statistical results of the particle size distribution from the data of Figure 2 are listed in Table I. It is

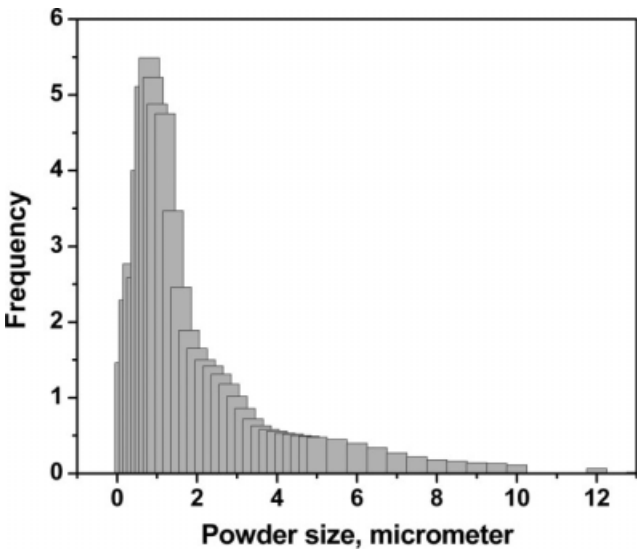


**Figure 2** Particle size distribution of superfine down powder.

**TABLE I**
**Statistical Results of the Particle Size Distribution**

| Item | Down fiber powder |
|---|---|
| Mean size (μm) | 1.546 |
| Standard deviation | 0.699 |
| Variance (μm) | 0.488 |
| Variance coefficient | 0.316 |
| Standard error | 0.452 |

evident that the mean powder size was 1.546 μm with a standard error and deviation of 0.452 and 0.699, respectively.

## FTIR analysis

FTIR spectra of the down fiber and down powder are shown in Figure 3. The two curves exhibit similar absorption bands around 3285 (N—H and O—H), 2870 (—$CH_2$), 1640 (amide I), 1520 (amide II), and 1230 $cm^{-1}$ (amide III). These bands are similar to the FTIR spectra of wool fiber[14] because both the down and wool fiber have large amounts of keratins; their chemical structures are much the same. Figure 3 also indicates that no new functional groups or chemical bonds were produced in the down powder after the milling process.

The peaks of the down powder around 1640, 1520, and 1230 $cm^{-1}$ are sharper than those of the down fiber; this may due to the changes in some amic groups during the milling. Usually, from 1000 to 1300 $cm^{-1}$, the spectra are characterized by the presence of medium-to-high intensity bands attributable to the different sulfur-containing chemical groups of keratin;[14] the sharper peak at 1230 $cm^{-1}$ indicates some changes in sulfur-containing groups during the milling process.

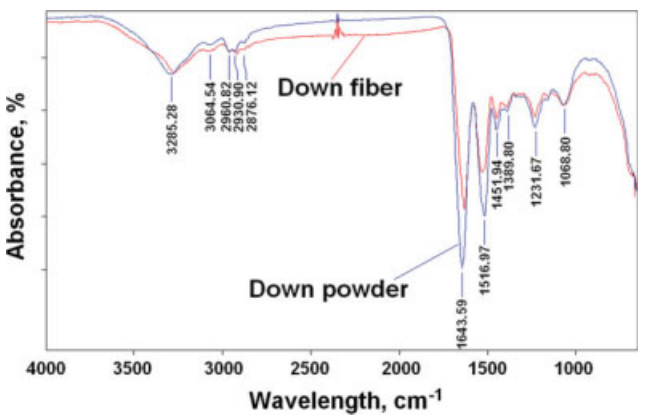


**Figure 3** FTIR spectra of down fiber and superfine down powder (600–4000 $cm^{-1}$). [Color figure can be viewed in the online issue, which is available at www.interscience.wiley.com.]

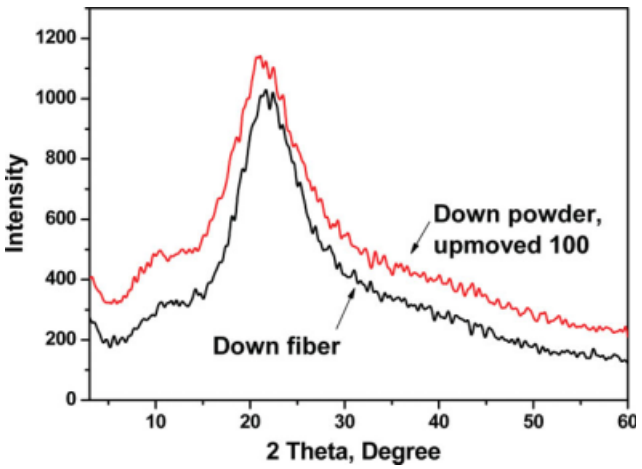


**Figure 4** X-ray diffraction curves of down fiber and superfine down powder. [Color figure can be viewed in the online issue, which is available at www.interscience.wiley.com.]

## X-ray diffraction analysis

X-ray diffraction curves of the down fiber and down powder are shown in Figure 4; they show a typical diffraction pattern of α-keratins with a prominent 2θ peak at 22° and a minor peak at 10° corresponding to the crystalline spacings of 4.39 and 9.82 Å, respectively.[13,14] The peak around 10° is characteristic of the hydrated crystalline structure of the protein fiber.[14] When the down fiber was ground into the down powder, the surface area increased, and thus it absorbed more water; a large number of water molecules were then joined onto the polar group of the fiber, and thus more hydrogen bonds were formed. Therefore, the peak at 10° of the down powder is more obvious than that of the down fiber, as shown in Figure 4. On the other hand, the peak at 20° of the down powder is lower and blunter than that of the down fiber, and this indicates that the crystallinity of the down powder is a little lower than that of the down fiber. Probably in the beginning of the grinding, some of the large crystals were destroyed, and the small crystals that were left were difficult to destroy by grinding. When silk fibers were ground into a superfine silk powder, the crystallinity dropped dramatically from 21.3% to 9.1%.[15] Compared with the silk powder, the wool fiber kept a more amorphous region, and the crystallinity of the wool powder decreased slightly versus that of the silk powder.

## Thermal analysis

TG curves of the down fiber and down powder are shown in Figure 5. There are two obvious weight-loss steps that correspond to the evaporation of water and thermal decomposition of the samples, and the residues of the two samples were almost the same.

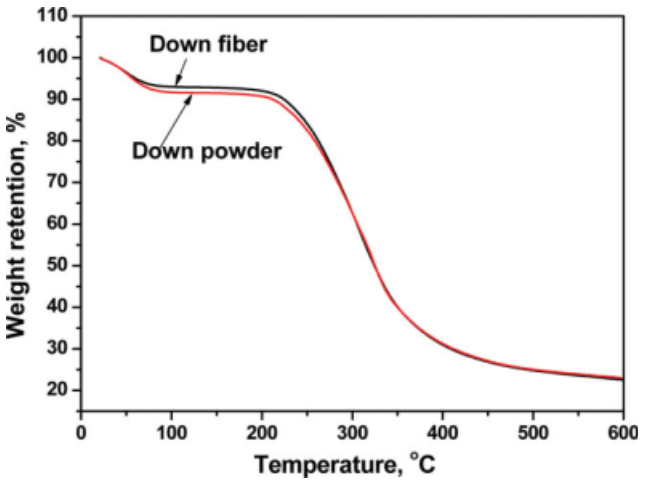


**Figure 5** TG curves of down fiber and superfine down powder. [Color figure can be viewed in the online issue, which is available at www.interscience.wiley.com.]

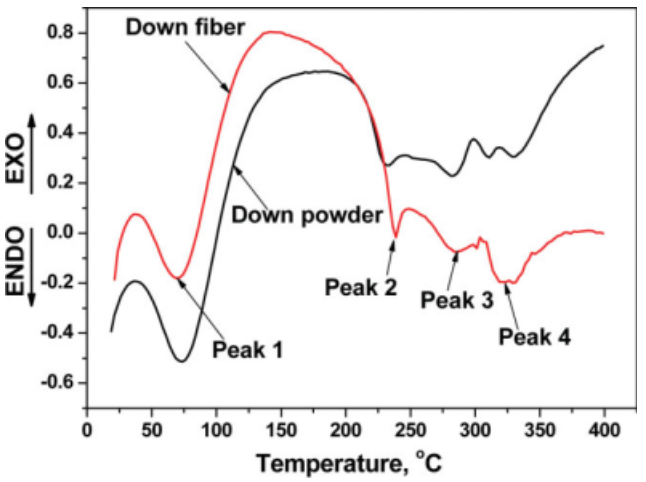


**Figure 7** DSC curves of down fiber and superfine down powder. [Color figure can be viewed in the online issue, which is available at www.interscience.wiley.com.]

Figure 6 amplifies the weight-loss steps of the TG curves; it is obvious that the down powder lost more weight than the down fiber in the first step. When the down fiber was ground into the superfine down powder, most crystals cleaved, and the crosslinks broke; this made larger amorphous regions for the powder. At the same time, the surface area increased greatly, so the powder absorbed more water; this meant that the powder had a higher first-step weight loss in the TG curve.

The initial temperature of the thermal decomposition stage is usually used to compare the thermal stability of samples. According to Figure 6, the initial temperatures of the down fiber and down powder were 243.4 and 242.5°C, respectively. Evidently, the thermal stability decreased when the down fiber was processed into the down powder. Unlike the superfine down powder, the initial temperature of the superfine silk powder increased slightly.[15]

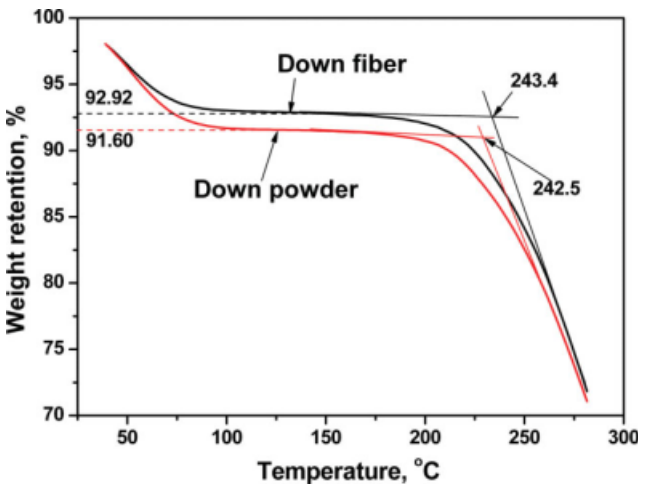


**Figure 6** First-step weight loss and initial decomposition temperature in the TG curves of down fiber and superfine down powder. [Color figure can be viewed in the online issue, which is available at www.interscience.wiley.com.]

DSC curves of the down fiber and down powder are shown in Figure 7, and they roughly correspond to two evident weight losses in the TG curves. According to some previous studies,[13,16,17] the four peaks can be explained as follows: peak 1 corresponds to the vaporization of bound water; peak 2 can be ascribed to crystal cleavage; peak 3 can be attributed to the breakdown of crosslinks, such as hydrogen bonds and salt bonds; and peak 4 corresponds to the rupture of peptide bonds, which leads to liquefaction.

Compared with the intensity of the peaks of the superfine down fiber, the intensity of peaks 2 and 3 decreased; this was probably due to changes in the crystals and the reduction of the crystallinity. As mentioned before, a large area of crystals broke during the grinding, and this made the thermal decomposition of the down powder easier than that of the down fiber; crosslinks in the structure of the keratins in the down could also be destroyed, and this also affected the thermal properties of the down powder. From Figure 7, we also found that the temperature of peak 3 of the down powder was a little lower than that of the down fiber; this certified the decrease in the thermal stability, just like the TG analysis. Two peaks around 320°C were found in the DSC curve of the down powder; however, the intensities of these peaks were much lower than that of peak 4, and this suggests that the superfine down powder could thermally decompose more easily than the down fiber.

## CONCLUSIONS

Down fiber was successfully ground into a superfine down powder on a purpose-built milling machine.

SEM photographs showed that the down fiber was ground into small particles on a microscale, and most of the particles had a rod shape. Particle size distribution analysis showed that the size of most of the powder was distributed around 0–3 μm, and the average size of the down powder was 1.546 μm. FTIR analysis showed there was no obvious change after the grinding; the peaks of the down powder around 1640, 1520, and 1230 $cm^{-1}$ were sharper than those of the down fiber, and this was probably due to the changes in some amic groups during the milling. X-ray diffraction analysis showed that the crystallinity of the superfine down powder was a little lower than that of the down fiber. TG analysis showed that the initial temperature of thermal decomposition decreased when the down fiber was ground into the powder. DSC analysis suggested that the intensity of the heat-absorbing peaks of the down powder was a little lower than that of the down fiber, and this suggested that the down powder could easily decompose.

## References


1. Yao, J.; Masuda, H.; Zhao, C.; Asakura, T. Macromolecules 2002, 35, 6.
2. Lock, R. L. U.S. Pat 5,252,285 (1993).
3. Lu, X.; Akiyama, D.; Hirabayashi, K. J Seric Sci Jpn 1994, 63, 21.
4. Takeshita, T.; Ishida, K.; Kamiishi, Y. Macromol Mater Eng 2000, 283, 126.
5. Otoi, K.; Horikawa, Y. U.S. Pat. 4,233,212 (1980).
6. Tsubouchi, K. U.S. Pat. 5,853,764 (1998).
7. Freddi, G.; Tsukada, M.; Beretta S. J Appl Polym Sci 1999, 71, 1563.
8. Tanaka, T.; Tanigami, T.; Yamaura, K. Polym Int 1998, 45, 175.
9. Kawahara, Y.; Shioya, M.; Takaku, A. Am Dyestuff Reporter 1996, 85(9), 88.
10. Pavlath, A. E.; Houssard, C.; Camirand, W. Text Res J 1999, 69, 539.
11. Li, Y.; Xu, W. U.S. Pat. 7,000,858 (2004).
12. Xu, W.; Cui, W.; Li, W.; Guo, W. Powder Technol 2003, 140, 136.
13. Xu, W.; Guo, W.; Li, W. J Appl Polym Sci 2003, 87, 2372.
14. Xu, W.; Ke, G.; Wu, J.; Wang, X. Eur Polym J 2006, 42, 2168.
15. Cui, W.; Liu, X.; Shen, X.; Peng, X.; Xu, W. Res J Text Apparel 2008, 12(2), 23.
16. Menefee, E.; Yee, G. Text Res J 1965, 36, 801.
17. Falix, W. D.; McDowall, M. A.; Eyring, H. Text Res J 1963, 33, 465.